

Central Force Optimization Technique based Harmonic Mitigation in Shunt Active Power Filters

M. Madhusudhan Reddy¹, P. Srinivasa Varma², D. Lenine³

Submitted: 10/09/2022 Accepted: 20/12/2022

Abstract: The Central Force Optimization Technique (CFOT) is used in this research to provide a novel way for compensating reactive powers and reducing harmonics in shunt active power filters (SAPF), resulting in a better proportional and integral (PI) gain. CFOT provides better accuracy than swarm intelligence techniques and other optimization methods. It also gives better and easier computational procedures. The performance of the proposed controller is validated using results obtained through Matlab. In order to prove the efficacy of the technique the results achieved are compared with nature-inspired controllers like Ant Colony optimization Algorithm (ACA) and Particle Swarm optimization (PSO) techniques. Various parameters such as total harmonic distortion (THD), active & reactive powers are utilized for the comparison purposes.

Keywords: Central Force Optimization Technique (CFOT), Ant Colony Optimization algorithm (ACA), Active Power Filter (SAPF), Particle Swarm Optimization (PSO).

I Introduction

The gap seen between quality of power delivered and the quality of power necessary for the load apparatus to operate consistently can be regarded as a power quality problem. Over the years, a variety of power enhancement devices have been created to safeguard equipment against power outages [1]. The following are some examples of effective and cost-efficient measures namely devices for power conditioning and specialized power sources. Lightning and surge arrestors, Transient Voltage Surge Capacitors, Filters, Isolation transformer, Voltage Regulators and Uninterruptible Power Supply are some of the power conditioning devices. SAPF is one of such power conditioning device which provides better power quality [2]. The pollution of AC supply systems can be caused by a variety of factors, including natural ones like lightning, flashover, equipment failure, and faults, as well as forced ones such voltage distortions and notches. Because they draw non-sinusoidal current and behave as nonlinear loads, a lot of customer's equipment pollutes the supply system. As a result, power quality is measured in

terms of the supply system's voltage, current, or frequency deviance, which can lead to equipment failure or malfunction. Voltage harmonics, surges, spikes, notches, sag/dip, swell, unbalance, fluctuations, glitches, flickers, outages, and so on are typical power quality issues related to the voltage at the point of common coupling (PCC) where multiple loads are connected [3]-[6].

These issues might occur in the supply system as a result of various system disruptions or the existence of nonlinear loads such as furnaces, uninterruptible power supplies (UPSs), and variable speed drives. Poor power factor, reactive power burden, harmonic currents, unbalanced currents, and an excessive neutral current in poly phase systems due to unbalancing and harmonic currents created by some nonlinear loads are some power quality issues connected to the current pulled from the AC mains. These power quality issues result in capacitor bank failure, increased distribution system and electric machine losses, noise, vibrations, over voltages and excessive current due to resonance, negative sequence currents in generators and motors, especially rotor heating, dielectric breakdown, communication system interference, relay and breaker malfunctions, false metering, interferences to the motor controllers and digital controllers among other things [7].

During each half cycle, however, some loads cause the current to change disproportionately with the voltage. Non-linear loads are what they're called. These non-linear loads cause current and voltage harmonics to be created. Non-sinusoidal current causes a variety of issues for utilities and power supply companies, including low power factor, low energy efficiency, electro-magnetic interference (EMI), power system voltage fluctuations, and so on. To avoid the harmful effects of harmonics, a perfect

¹Research Scholar, Dept. of EEE, KoneruLakshmaiah Education Foundation, Vaddeswaram, A.P, India

mmsr244@gmail.com,

² Associate Professor, Dept. of EEE, KoneruLakshmaiah Education Foundation, Vaddeswaram, A.P, India

pinnivarma@gmail.com

³ Professor, Dept. of EEE, RGM College of Engineering & Technology,

Nandyal, A.P, India

lenine.eee@gmail.com

Other Recommendations

¹ mmsr244@gmail.com

² pinnivarma@gmail.com

³ lenine.eee@gmail.com

compensator is required [8]. The gap seen between qualities of power delivered and the quality of power necessary for the load apparatus to operate consistently can be regarded as a power quality problem. Over the years, a variety of power enhancement devices have been created to safeguard equipment against power outages. The following are some examples of effective and cost-efficient measures namely devices for power conditioning and specialized power sources. Lightning and surge arrestors, Transient Voltage Surge Capacitors, Filters, Isolation transformer, Voltage Regulators and Uninterruptible Power Supply are some of the power conditioning devices [9]-[12]. SAPF is one of such power conditioning device which provides better power quality. The SAPF is controlled by any one or combinations of controllers to draw or supply compensating current from or to the load respectively to cancel out current harmonics on the AC side, and to keep the DC link voltage constant by keeping the real power flow in the system and reactive power flow from or to the source, putting the source current in phase with the source voltage [13]. The active power filter's basic compensation principle is shown in Figure 1, and it acts as an energy storage element to supply the real power difference between the load and the source during the transient period. The real power in the system, i.e. the power between the mains and the load, changes as the load state changes. The faulty functioning of the system occurs as a result of the real power imbalance, and the real power disturbance is cleared by the DC link capacitor, causing the voltage across the DC link capacitor to change away from the reference voltage [14]-[16].

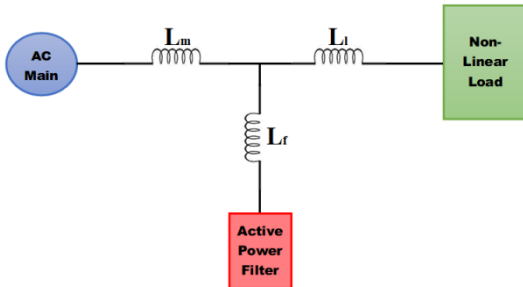


Figure 1. General Structure of Active Filters

The CFO Tmetaheuristic optimization is a new optimization evolutionary algorithm (EA). CFOT looks for the extrema of an optimization problem to maximize in a multivariate search area. It is based on a gravitational pull similarity to classical particle kinematics. A metaheuristic, by definition, is a set of algorithmic notions that can be used to build heuristic techniques for a variety of situations. To put it another way, a metaheuristic is a broad sense computational architecture that may be used to solve a variety of optimization problems with few changes. A metaheuristic is usually proposed without any mathematical proof, and it is frequently inspired by a biological metaphor, with ACA and PSO being notable instances [17]. CFOT is proposed in the same way, however it is based on an analogy drawn from the motion of masses in a gravitational field rather than biology. Not much applications of CFOT in the power system network are available in the literature. This paper will be focusing

on exploration of a new area for the CFO methodology. It is used in the SAPF as a novel controller, which enhances the power quality as compared to the other methods viz. ACA & PSO.

II Central Force Optimization Methodology

Unlike other extensively used metaheuristics, CFOT is fundamentally deterministic. By analogy to masses moving under the influence of gravity, it models probes that fly through the decision space. Using the example of particle motion in a gravity pull, models characterizing the probes' locations and accelerations are derived. Objects travelling through three-dimensional space become locked in close orbits around highly gravitational masses in the physical universe, which is similar to finding the maximum value of an objective function.

The algorithm is deterministic since CFOT lacks randomization properties. CFOT models are based on the concept of probes moving through space. One probe will be attracted by another probe of equal or larger mass, but the heavier probe will be unaffected. The probes are modelled using known equations with a focus on physical features, allowing their journey to be duplicated with no subsequent random modifications. The probes positions and accelerations will be updated on a regular basis. The procedure will be repeated until a global optimum solution is discovered [18]-[22].

A group of probes is represented as a potential solution in CFO, with each probe 'p' having a position vector $P^p(t)$ & an acceleration vector $A^p(t)$ at time t.

The acceleration vector is updated using the following equation.

$$A_i^p(t) = G \sum_{\substack{j=1 \\ j \neq p}}^{n_p} U(F^j(t) - F^p(t)) (F^j(t) - F^p(t)) \frac{(P_i^j(t) - P_i^p(t))^\alpha}{\|P^j(t) - P^p(t)\|^\beta} \quad - (1)$$

Probe p's position is updated using the following equation.

$$P_i^p(t+1) = P_i^p(t) + \frac{A_i^p(t) \Delta t^2}{2} \quad - (2)$$

Here

G – represents the Gravitational constant

$F^k(t) = fit(R^k(t))$ gives the fitness value of the probe k's position at time

't', where $(k = 1, 2, \dots, n_p)$

n_p – number of initial probes

α, β – are CFOT parameters

U – Unit step input, $U(s) = 1$ for $s \geq 0$ or else it is equal to zero.

Δt – represents the unit step increment of time.

$$\|P^j(t) - P^p(t)\| = \sqrt{\sum_{i=1}^{n_d} (P_i^j(t) - P_i^p(t))^2}$$

n_d – represents the number of variables in the decision space (D_s)

$D_s = \{a_1, a_2, \dots, a_{n_d}\}$, within the limits given by $P_i^{min} \leq a_i \leq P_i^{max}$

If the generated probe is beyond the D_s , then positions of the probes are reassigned as given by the following equations (3) and (4).

If the position is below the lower limit P_i^{min} , then it is repositioned as given by the equation (3),

$$P_i^p(t+1) = P_i^{min} + P_{new}[P_i^p(t-1) - P_i^{min}] \quad - (3)$$

If the position is above the upper limit P_i^{max} , then it is repositioned as given by the equation (4),

$$P_i^p(t+1) = P_i^{max} - P_{new}[P_i^{min} - P_i^p(t-1)] \quad - (4)$$

Here P_{new} is known as the reposition factor.

The steps involved in the CFOT process is given below

1. For each probe, define an initial position and zero acceleration.
2. For each probe, calculate the value of P and choose the place with the highest P.
3. Compute the new position of the probes, $P_i^p(t+1)$. If it exceeds the Ds limit then adjust the position by the equations (3) & (4).
4. Update P and locate the probe with the highest value.
5. Using Equation (1), update the acceleration of each probe.
6. Determine whether the convergence requirements are met. Return to step 3 if it does not fulfill.

The general flowchart of the proposed CFOT is described in the figure 2.

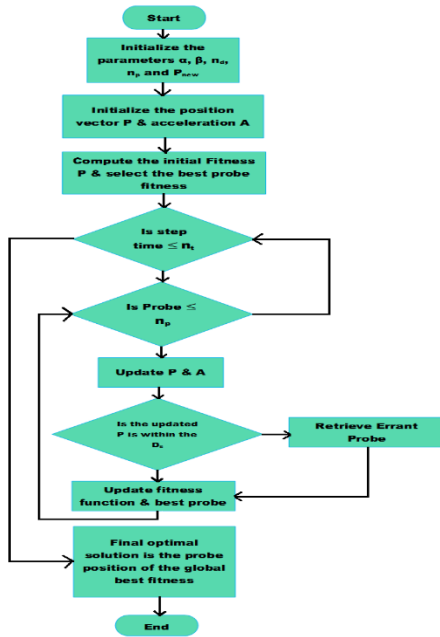


Figure 2. Flowchart of the proposed CFOT

III Design of Active Power Filter

After nonlinear application into the system, the p-q theory is used to improve the source current index. It essentially decreases lower-order harmonics in the power system. The instantaneous p-q theory creates compensatory signals based on the non-linear loads (NLL) actual and reactive power.

P-q theory is used to generate the reference signal. Clarke's transformation is used to convert a three-phase system to a two-phase system (abc- $\alpha\beta$). The real and reactive power of

the NLL are calculated using the converted numbers discussed below. The p-q quantities include both AC and DC components. The AC Component is extracted using the HPF, and the reference signal is calculated using the inverse transformation.

$$\begin{bmatrix} v_{s0} \\ v_{s\alpha} \\ v_{s\beta} \end{bmatrix} = \sqrt{\frac{2}{3}} \begin{bmatrix} \frac{1}{\sqrt{2}} & \frac{1}{\sqrt{2}} & \frac{1}{\sqrt{2}} \\ 1 & -\frac{1}{2} & -\frac{1}{2} \\ 0 & \frac{\sqrt{3}}{2} & -\frac{\sqrt{3}}{2} \end{bmatrix} \begin{bmatrix} v_{sa} \\ v_{sb} \\ v_{sc} \end{bmatrix} \quad - (5)$$

$$\begin{bmatrix} i_{L0} \\ i_{L\alpha} \\ i_{L\beta} \end{bmatrix} = \sqrt{\frac{2}{3}} \begin{bmatrix} \frac{1}{\sqrt{2}} & \frac{1}{\sqrt{2}} & \frac{1}{\sqrt{2}} \\ 1 & -\frac{1}{2} & -\frac{1}{2} \\ 0 & \frac{\sqrt{3}}{2} & -\frac{\sqrt{3}}{2} \end{bmatrix} \begin{bmatrix} i_{La} \\ i_{Lb} \\ i_{Lc} \end{bmatrix} \quad - (6)$$

The instantaneous active power (p), reactive power (q), and zero sequence power (p0) are all expressed in equation (7).

$$\begin{bmatrix} p_0 \\ p \\ q \end{bmatrix} = \begin{bmatrix} v_{s0} & 0 & 0 \\ 0 & v_{s\alpha} & v_{s\beta} \\ 0 & v_{s\beta} & -v_{s\alpha} \end{bmatrix} \begin{bmatrix} i_{L0} \\ i_{L\alpha} \\ i_{L\beta} \end{bmatrix} \quad - (7)$$

The following equations (7) & (8) gives the active and reactive power using the p-q approach from Clarke translation

$$p = \bar{p} + \tilde{p} \quad - (8)$$

$$q = \bar{q} + \tilde{q} \quad - (9)$$

Here, \bar{p} and \bar{q} represents the DC average value of instantaneous real & imaginary part of the signal and \tilde{p} and \tilde{q} represents AC value of instantaneous real & imaginary part of the signal.

The reference currents in $\alpha - \beta$ coordinates are given by the following equation number (10)

$$\begin{bmatrix} i_{c\alpha}^* \\ i_{c\beta}^* \end{bmatrix} = \frac{1}{v_{s\alpha}^2 + v_{s\beta}^2} \begin{bmatrix} v_{s\alpha} & v_{s\beta} \\ v_{s\beta} & -v_{s\alpha} \end{bmatrix} \begin{bmatrix} -\bar{p} + \overline{\Delta p} \\ -q \end{bmatrix} \quad - (10)$$

Additional average power is required to compensate for VSI losses caused by the switching of power electronics switches, and it is given as

$$\overline{\Delta p} = \bar{p}_0 + \overline{p_{loss}} \quad - (11)$$

Here $\overline{p_{loss}}$ represents average losses in the inverter. The error is passed to the PI controller for further processing once the actual DC-link capacitor voltage (Vdc) and reference value (Vdc*) are compared.

$$\begin{bmatrix} i_{ca}^* \\ i_{cb}^* \\ i_{cc}^* \end{bmatrix} = \sqrt{\frac{2}{3}} \begin{bmatrix} \frac{1}{\sqrt{2}} & 1 & 0 \\ \frac{1}{\sqrt{2}} & -1 & \frac{\sqrt{3}}{2} \\ \frac{1}{\sqrt{2}} & \frac{1}{2} & -\frac{\sqrt{3}}{2} \end{bmatrix} \begin{bmatrix} -i_0 \\ i_{ca}^* \\ i_{cb}^* \end{bmatrix} \quad - (12)$$

v_{sa}' , v_{sb}' , and v_{sc}' are used in transformations for 3-phase three wire system, which is given by equation (13), v_{α}' , v_{β}' are used in transformations for three phase four wire system, which is given by equation (14).

$$\begin{bmatrix} v_{sa}' \\ v_{sb}' \\ v_{sc}' \end{bmatrix} = \sqrt{\frac{2}{3}} \begin{bmatrix} 1 & 0 \\ -1 & \frac{\sqrt{3}}{2} \\ \frac{1}{2} & -\frac{\sqrt{3}}{2} \end{bmatrix} \begin{bmatrix} v_{\alpha}' \\ v_{\beta}' \end{bmatrix} \quad - (13)$$

$$\begin{bmatrix} v_{\alpha}' \\ v_{\beta}' \end{bmatrix} = \frac{1}{\sqrt{i_{\alpha}'^2 + i_{\beta}'^2}} \begin{bmatrix} i_{\alpha}' & -i_{\beta}' \\ i_{\beta}' & i_{\alpha}' \end{bmatrix} \begin{bmatrix} p' \\ q' \end{bmatrix} \quad - (14)$$

The proposed control schematic of the CFOT methodology is shown in the figure 3.

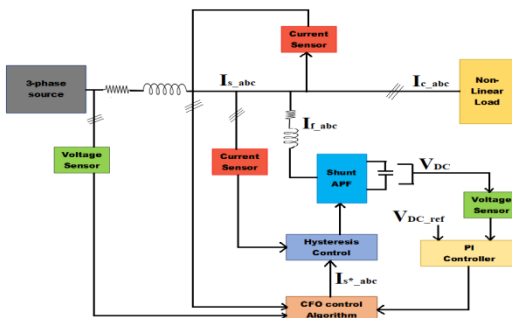


Figure 3. Block diagram of proposed CFO-PI Controller

IV Results and discussions

The simulation results obtained through Matlab are discussed in this section. Simulation is carried out for the proposed CFOT based controller and also for PSO and ACA based controllers and all the results are compared. The parameters used for the simulation purposes are tabulated in table 1.

Parameter	Values
Grid Voltage	415 Volt
Source Resistance (R_s)	0.1 ohm
Source Inductance (L_s)	0.15 milli Henry
Load Resistance (R_l)	100 ohm
Load Inductance (L_l)	200 milli Henry

Table 1: Simulation parameters

The following figures depict the waveforms obtained from the simulation results. Various graphs like source current, source voltage, output current, output voltage, THD, active & reactive powers and filter capacitance voltage were all recorded for the comparison parameters in order to prove

the efficacy of the proposed CFOT controller against the PSO and ACA controllers

The three phase source current, i.e. the grid current and output current of the PSO, ACA and CFOT based systems, are shown in figures 4, 5 & 6 respectively and is sinusoidal in all the three cases. The changes of the output three phase voltages and currents for all the three types of controllers are depicted in Figures 7 to 9. The three phase input voltages and currents for PSO, ACA and CFOT controllers are shown in Figures 10, 11 and 12 correspondingly. It can be seen that the oscillations settle fast, resulting in a reduction in THD.

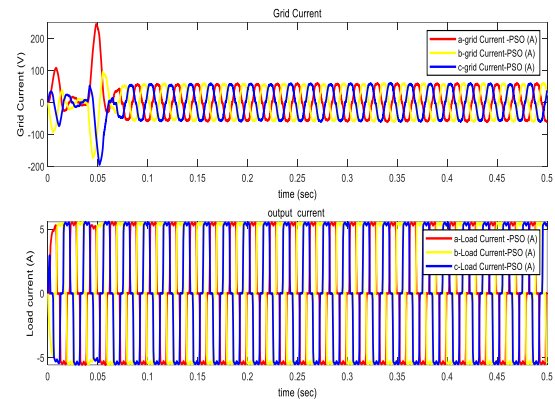


Figure 4. Waveform of a) source current and b) output current for PSO based controller

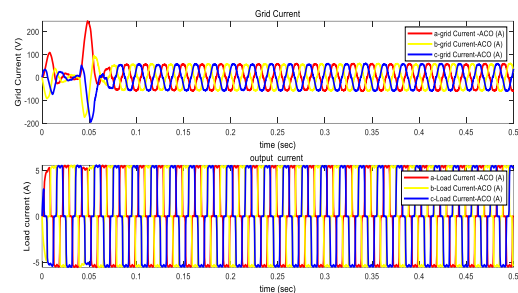


Figure 5. Waveform of a) source current and b) output current for ACA based controller

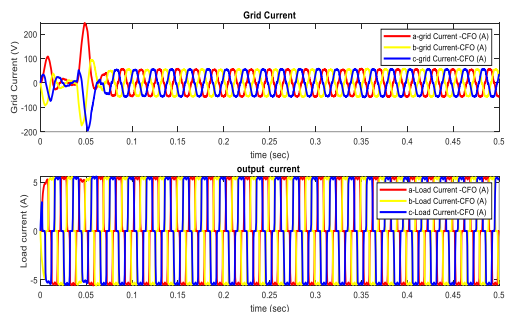


Figure 6. Waveform of a) source current and b) output current for CFOT based controller

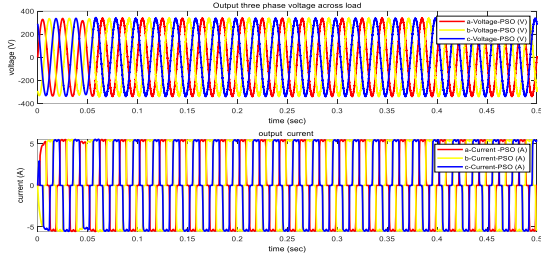


Figure 7. Waveform of O/p voltage & current for PSO controller

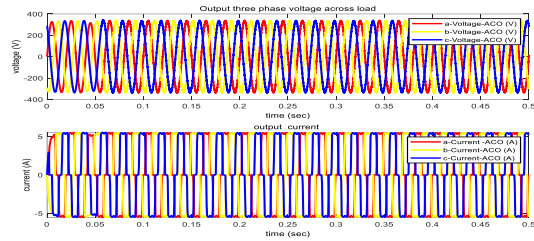


Figure 8. Waveform of O/p voltage & current for ACA controller

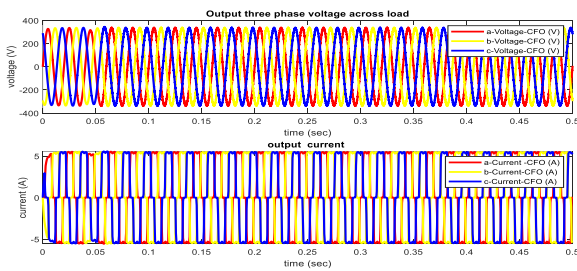


Figure 9. Waveform of O/p voltage & current for CFOT

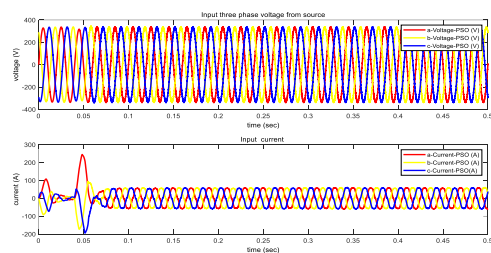


Figure 10. Waveform of input voltage and current for PSO based controller

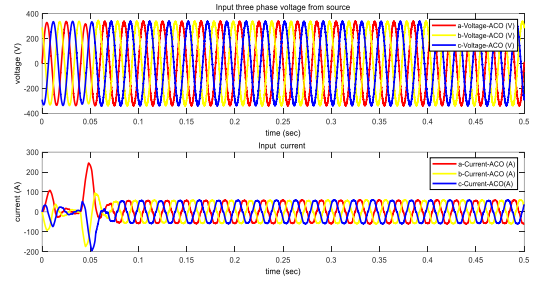


Figure 11. Waveform of input voltage and current for ACA based controller

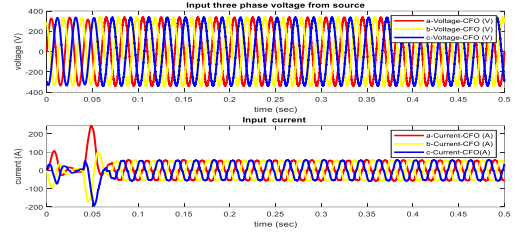


Figure 12. Waveform of input voltage and current for CFOT based controller

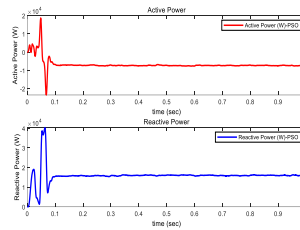


Figure. 13 a)

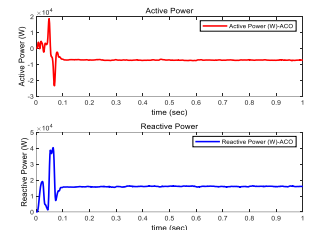


Figure. 13 b)

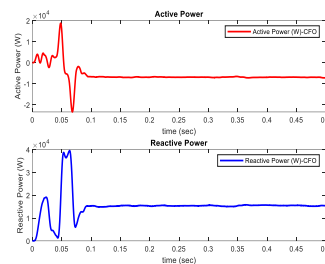


Fig. 13 c)

Figure 13. Waveforms showing the active and reactive powers for a) PSO b) ACA c) CFOT

Figures 13 shows the active and reactive powers corresponding to each controllers. Figure 14 shows the source current waveforms and their accompanying THD for the PSO trained controller. The PSO-based controller has a THD of 2.48 percent, which is substantially below the IEEE standard. Similarly the source currents waveforms and its corresponding THD for the ACA and CFOT controllers are displayed in the figures 15 and 16 respectively. The THD for ACA controller seems to be 2.15 % and for that of the proposed CFOT method it is 1.95 % which is less than the other two techniques. Table 2 lists the comparative

performances parameters of all the 3 methods taken in this research work.

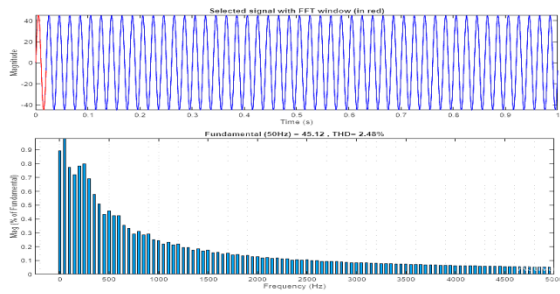


Figure 14. Waveform of a) source current and b) THD of source current for PSO based controller

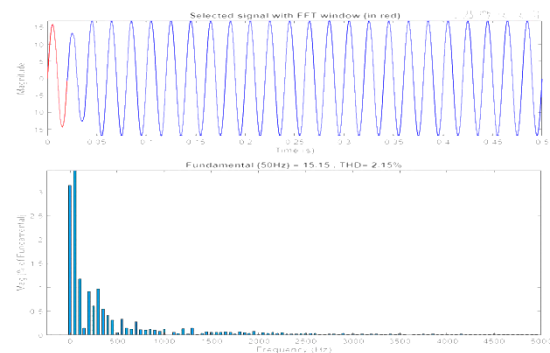


Figure 15. Waveform of a) source current and b) THD of source current for ACA based controller

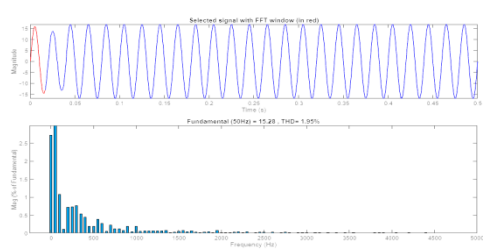


Figure 16. Waveform of a) source current and b) THD of source current for CFOT based controller

Type of Controller	% THD	Active power	Reactive power
PSO controller	2.48 %	5579	198.4
ACA controller	2.15 %	5860	125.4
CFOT controller	1.95 %	6061	25.02

V Conclusions

A novel Central Force Optimization Technique is proposed for the power quality improvement in the SAPF based power network which contains non-linear loads. The harmonics

generated due to the presence of the non linearities are compensated and the corresponding THD values are well below the standards. The robustness and the effectiveness of the proposed controllers are also well proved with the help of simulation results, as compared with that of the other optimization methods namely PSO & ACA based controllers.

References:

- [1] Anish PratapVishwakarma and Ksh. Milan Singh, "Comparative Analysis of Adaptive PI Controller for Current Harmonic Mitigation", International Conference on Computational Performance Evaluation (ComPE), North-Eastern Hill University, Shillong, Meghalaya, India. pages 644-648, 2020.
- [2] Rajeshwari and Ashish Bagwari, "Voltage Harmonic Reduction Using Passive Filter Shunt Passive-Active Filters for Non-Linear Load", 2017 7th International Conference on Communication Systems and Network Technologies (CSNT), IEEE, pages 131-136, 2017.
- [3] N. Gowtham, and Shobha Shankar, "PI Tuning of Shunt Active Filter Using GA and PSO Algorithm", 2nd International Conference on Advances in Electrical, Electronics, Information, Communication and Bio-Informatics (AEEICB), IEEE, pp. 20713, 2016.
- [4] M. Dorigo, G. DiCaro and L. M. Gambardella, "Ant algorithms for discrete optimization", Artificial Life Journal, vol. 5, pages 137-172, 1999.
- [5] Janga Reddy M, Nagesh Kumar D, "Evolutionary algorithms, swarm intelligence methods, and their applications in water resources engineering: a state-of-the-art review". H2OpenJ 3 135-188, 2020.
- [6] W. Huaisheng and X. Huifeng, "A novel double hysteresis current control method for active power filter," Physics Procedia, vol. 24, pp. 572–579, 2012.
- [7] W. Huaisheng and X. Huifeng, "A novel double hysteresis current control method for active power filter," Physics Procedia, vol. 24, pp. 572–579, 2012.
- [8] María Isabel Milanés Montero, Enrique Romero Cadaval and FermínBarrero González, "Comparison of Control Strategies for Shunt Active Power Filters in Three-Phase Four-Wire Systems", IEEE Transactions On Power Electronics, Vol. 22, No. 1, January 2007.
- [9] Suresh Mikkili and Anup Kumar Panda, "Real-Time Implementation of Shunt Active Filter P-Q Control Strategy for Mitigation of Harmonics with Different Fuzzy M.F.s", Journal of Power Electronics, Vol. 12, No. 5, September 2012.
- [10] Om. P. Mahela and A. GafoorShaik, "Topological aspects of power quality improvement techniques: A comprehensive overview", Renewable and Sustainable Energy Reviews, Volume 58, May 2016, Pages 1129-1142. DOI: 10.1016/j.rser.2015.12.251
- [11] Chelli, Z.; Toufouti, R.; Omeiri, A.; Saad, S. Hysteresis control for shunt active power filter under unbalanced three-phase load conditions. Journal of Electronics and Computer Engineering, 2015.
- [12] L. Kritele, B. Benhala, and I. Zorkani, "Ant Colony Optimization for Optimal Analog Filter Sizing", Chapter 10, Book: Focus on swarm intelligence research and applications, Eds., B. Benhala, P. Pereira and A. Sallem, NOVA Science Publishers, pages 193–220, 2017.
- [13] Mai Diab, Mohamed El-Habrouk, Tamer H. Abdelhamid and Samir Deghedie, "Switched Capacitor Active Power Filter Optimization Using Nature-Inspired Techniques", 21st International Middle East

- Power Systems Conference (MEPCON), Tanta University, Egypt, Volume 1, pages 556-561, 2019
- [14] Z. Y. Li, Z. Ren, Z. M. Y., "Survey on Active Power Filter Devices and Their Application Study", *Power System Technology*, vol. 28, no. 22, pages 40-43, 2004.
- [15] W. Wang, Y. Ling and J. Zhang, "Ant colony optimization algorithm for design of analog filters", *WCCI 2012 IEEE World Congress on Computational Intelligence*, Brisbane Australia, June 2012.
- [16] A. Dubey, S. P. Dubey and L. Sahu, "PSO based hybrid active filter for harmonic and reactive power compensation", *International Conference Shashtrarth*, 2013.
- [17] R. A. Formato, "Central Force Optimization: A New Metaheuristic with Applications In Applied Electromagnetics", *Progress In Electromagnetics Research (PIER)*, Vol. 77, pp. 425-491, 2007.
- [18] R. C. Green, L. Wang, M. Alam, and R. A. Formato, "Central Force Optimization on a GPU: A case study in high performance metaheuristics using multiple topologies," in *2011 IEEE Congress of Evolutionary Computation (CEC)*, 2011, no. 2, pp. 550-557.
- [19] I. Amaya, J. Cruz, and R. Correa, "Solution of the Mathematical Model of a Nonlinear Direct Current Circuit Using Particle Swarm Optimization," *Revista Dyna*, vol. 79, no. 172, pp. 77-84, 2012.
- [20] LIU Jie, "Adaptive Central Force Optimization with Variable Population Size", *10th International Conference on Computational Intelligence and Security*, pp. 17-20, 2014.
- [21] L. Jie, W. Y. Ping, "An improved central force optimization based on simplex method," *Journal of Zhejiang University (Engineering Science)*, vol. 48, pp. 2116-2122, 2014.
- [22] L. Jie, W. Yuping, "Central Force Optimization with Self-Adaptive Control Strategy of Population Size," *Journal of Beijing University of Posts and Telecommunications*, vol. 38, pp. 15-19, 2015.
- [23] M. Dorigo, M. Birattari, and T. Stutzle, "Ant colony optimization," *IEEE Computational Intelligence Magazine*, vol. 1, no. 4, pp. 28-39, 2006.
- [24] X.-S. Yang and S. Deb, "Engineering optimisation by cuckoo search," *International Journal of Mathematical Modelling and Numerical Optimisation*, vol. 1, no. 4, pp. 330-343, 2010.
- [25] Yao, X., Y. Liu, and G. Lin, "Evolutionary programming made faster," *IEEE Trans. Evolutionary Computation*, Vol. 3, No. 2, 82-102, Jul. 1999.